AJNR

3D Cerebral Angiography: Radiation Dose Comparison with Digital Subtraction Angiography

Beth A. Schueler, David F. Kallmes and Harry J. Cloft

3D Cerebral Angiography: Radiation Dose Comparison with Digital Subtraction Angiography

Beth A. Schueler, David F. Kallmes, and Harry J. Cloft

BACKGROUND AND PURPOSE: As the use of 3D rotational angiography (3D RA) for the evaluation of cerebral vasculature becomes more widespread, it is important to evaluate this imaging method's effect on patient radiation dose. The purpose of the study is to measure 3D RA radiation dose as compared with biplanar digital subtraction angiography (DSA).

METHODS: The distribution and peak skin dose were measured for 3D RA and biplanar DSA by using an anthropomorphic skull phantom. In addition, the cumulative incident dose, summed over all images in each acquisition, was determined. Measurements were acquired for our facility's standard 3D RA acquisition mode (25°/s rotational speed; 162 total frames) and other available acquisition mode selections.

RESULTS: For 3D RA, the skin dose was found to be distributed across the back and sides of the skull with the peak skin dose located at the center of the back of the skull. The peak skin dose for the standard 3D RA acquisition mode was 15 mGy. For a biplanar DSA run, the peak skin dose was 58 mGy, also located at the back of the skull. The cumulative incident dose for the standard 3D RA acquisition mode was 33 mGy, compared with 53 mGy for biplanar DSA.

CONCLUSION: The patient radiation dose for 3D RA is significantly lower than for biplanar DSA, by nearly a factor of 4 in peak skin dose and 40% lower in cumulative incident dose.

3D rotational angiography (3D RA) has become a critical imaging tool in neuroradiology, allowing for the visualization of detailed cerebral vasculature in nearly real time. Because of recent advances in C-arm gantry movement and reconstruction algorithm speed, 3D RA has grown from a novel, experimental technique into a routine clinical imaging method. Specific evidence of the clinical benefits of 3D RA, particularly for imaging cerebral aneurysms, is detailed in recent publications by Klucznik (1) and others (2–8).

From numerous reports (9–13) and a US Food and Drug Administration advisory (14), it is known that patient dose in neurointerventional procedures can be high and that radiation-induced skin injuries are possible. One might expect that the radiation dose associated with 3D RA is high as compared with biplanar digital subtraction angiography (DSA), because the number of frames required to produce a 3D

RA volume reconstruction (100–300 frames) is much higher than a typical biplanar series (20–40 frames). X-ray technique factors (including beam energy, milliamprage, and exposure time per frame) for the 2 types of image acquisition differ, however, and the 3D RA entrance exposure area is spread over a larger region of the head. As a result, it is not immediately evident which imaging method poses a greater radiation exposure risk. In this study, we undertook to measure patient radiation dose associated with 3D RA of the head as compared with biplanar DSA.

Methods

Patient radiation dose was measured by simulating 3D RA and DSA acquisitions with an anthropomorphic skull phantom (Alderson Angiographic Head Phantom; Radiology Support Devices, Long Beach, CA) by using a biplanar angiography system (Neurostar Plus; Siemens Medical Solutions, Erlangen, Germany). The angiography system incorporates a 0.2-mm copper filter that is introduced into the x-ray beam automatically, depending on patient attenuation. Images were acquired for 3D RA by rotating the frontal C-arm in 2 arcs, 1 for mask acquisition and another with injection of contrast material. Image acquisition covered 100° left anterior oblique to 100° right anterior oblique with the x-ray tube traveling under the patient. Available rotation speed and dose mode selections are shown in Table 1. A shaped, aluminum form filter, supplied by the manufacturer, was placed in the x-ray beam for all 3D RA acquisitions. Dose measurements were made in the each of 6 acquisition modes by using the 30-cm image intensifier (II)

TABLE 1: 3D RA acquisition modes

Acquisition Mode	Rotational Arc Duration (s)	Rotational Speed (°/s)	Total Frames Acquired	Dose Mode
3D-L 5S	5	40	102	Low
3D-H 5S	5	40	102	High
3D-L 8S	8	25	162	Low
3D-H 8S	8	25	162	High
3D-L 14S	14	14	266	Low
3D-H 14S	14	14	266	High

TABLE 2: Biplanar DSA series acquisition parameters

C-arm	Frames	FOV	Angulation	kVp	Cu Filtration (mm)
Frontal	18	22-cm	20° CR	75	0
Lateral	18	22-cm	0° CR/CA	73	0.2

Note.—FOV indicates field-of-view; CR, cranial; CA, caudal.

field-of-view (FOV), 70 kVp, and no added copper filtration. The 3D-H 8S acquisition mode was generally used for 3D RA acquisitions at our facility.

For biplanar DSA, typical exposure technique parameters used at our facility were determined by reviewing 40 patient DSA series. The most commonly used acquisition parameter settings are shown in Table 2. In addition, the frontal and lateral plane DSA dose mode was set to 4.8 μGy II input dose per frame in the 17-cm FOV.

Dose Quantities

The biologic effects of radiation in neurointerventional procedures include deterministic effects (such as skin erythema and epilation) and stochastic effects (such as cancer induction and genetic effects). To assess the risk of skin injury, we compared the location and magnitude of the peak skin dose for 3D RA and biplanar DSA. The risk of stochastic effects can be estimated from the cumulative dose-area product (DAP), which is the product of the incident dose and x-ray field area summed over all segments of a procedure (15). The incident dose is defined as the air kerma (or absorbed dose in air) on the x-ray beam axis at the focus to skin distance. For 3D RA, however, the x-ray field area extends beyond the edges of the skull, whereas for biplanar DSA, the x-ray field area conforms to or is just within the skull boundary. As a result, the cumulative DAP for a 3D RA acquisition overestimates the patient area exposed and thus overestimates the risk of stochastic risk when compared with biplanar DSA. Alternatively, the cumulative incident dose provides a method of comparing stochastic risk from 3D RA with biplanar DSA because the same critical organs (brain and skull) are nearly fully exposed in both imaging acquisition techniques. For 3D RA, the cumulative incident dose is a total of the entrance skin air kerma for each frame acquired in the 2 rotational arcs. For biplanar DSA, the cumulative incident dose is the sum of the frontal and lateral entrance skin air kerma.

Peak Skin Dose

The distribution of the skin dose was recorded with direct exposure film (XV-2 Ready-Pak; Eastman Kodak, Rochester, NY) wrapped around the surface of the skull phantom. Once the location of the highest skin dose was determined, a skin dose monitor (SDM model 104–101; McMahon Medical, San Diego, CA) was used to measure the peak skin dose at that site and other sites on the phantom surface. The skin dose monitor

is a small, thin scintillation detector (16, 17) that can be placed at a specific location, including between the phantom and table pad, with minimal disruption of the phantom position.

Calibration of the skin dose monitor readout was conducted according to manufacturer specifications by using a reference ionization chamber (10X5-6 model) and radiation monitor (MDH 1015C; Radcal Corporation, Monrovia, CA). The x-ray beam energy parameters used for calibration (kVp and filtration) duplicated those used for the phantom peak skin dose measurement. It should also be noted that the skin dose monitor exhibits a drop in sensitivity when exposed at an angle of incidence >30° (17). X-ray beam directionality is inconsequential for the biplanar DSA acquisition, because the entrance beam direction is always 0°. For the 3D RA acquisition, however, the detector is exposed through a range of angles as the x-ray tube rotates through its arc. For the specific 3D RA acquisition geometry used in this study, the x-ray beam angle of incidence was found to be, at most, 45°, which results in an error of 10% for frames acquired at the largest angulation. Averaged over the entire rotational arc, the skin dose monitor error attributed to directionality is expected to be approximately 2%.

Cumulative Incident Dose

The cumulative incident dose was determined by using the angiography unit's integrated dosimeter, which incorporates a DAP transmission ionization chamber and electronic sensing of the collimator positions to measure reference air kerma. Reference air kerma (18) is defined as the air kerma on the x-ray beam axis at the interventional reference point located 15 cm from the system isocenter toward the focal spot (which corresponds to a focus to skin distance of 60 cm for the angiography system). The cumulative incident dose was calculated by correcting the reference air kerma value to the actual focus to skin distance, which ranged from 66 to 70 cm, depending on the C-arm angulation. The angiography unit's integrated dosimeter output was calibrated by using a reference ionization chamber (10X5-6 model) large enough to nearly cover the full x-ray beam cross-section. This calibration method allowed for correction of the nonuniform distribution of the x-ray beam caused by the shaped form filter. In addition, an air kerma correction factor for table and pad attenuation was also measured and applied to frames where the table and pad intercepted at least half of the x-ray field of view.

Results

Peak Skin Dose

The direct exposure film measurement of the skin dose distributions for 3D RA and biplanar DSA are shown in Fig 1. For 3D RA, the film optical attenuation distribution indicated that the location of the peak skin dose was the center of the back of the skull. Skin dose monitor measurements taken in the center of the left and right lateral projections indicated that the dose at these locations is approximately 50% of the peak skin dose. Table 3 lists the measured peak skin dose for each of the 6 3D RA acquisition modes. The high-dose mode acquisitions were found to be approximately 2.3 times higher in peak skin dose as compared with low-dose mode acquisitions for the same rotational arc duration. Also, the peak skin dose increases were roughly proportional to the rotation arc duration for the same dose mode.

For a biplanar DSA series, the film exposure indicated that the peak skin dose region was similarly located at the back of the skull. No overlap between
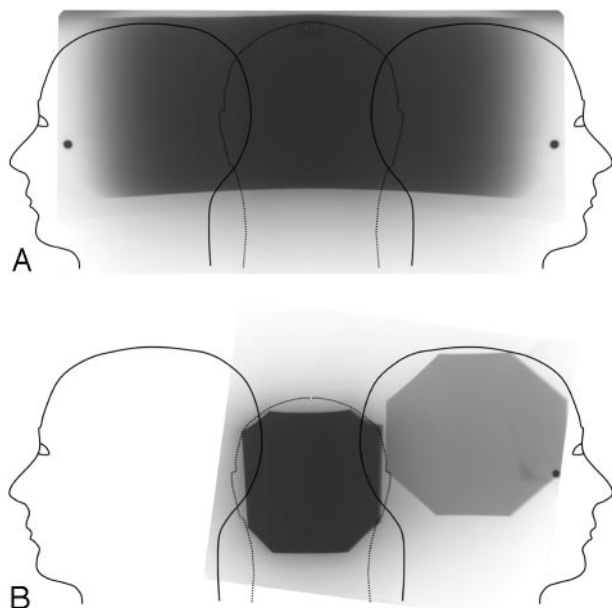
FIG 1. Skin dose distribution for (*A*) 3D RA and (*B*) biplanar DSA. The exposed film is overlaid on a graphic representation of skin surface unfolded from the anterior midline.

TABLE 3: 3D RA and biplane DSA peak skin dose and cumulative incident dose

Acquisition Mode	Peak Skin Dose (mGy)	Cumulative Incident Dose (mGy)
3D-L 5S	3.9	9.4
3D-H 5S	8.4	21
3D-L 8S	6.1	15
3D-H 8S	15	33
3D-L 14S	10	25
3D-H 14S	26	58
Biplane DSA	58	53

the frontal and lateral entrance exposure regions was found for the configuration used in this study. The measured peak skin dose for biplanar DSA was 58 mGy. At the center of the exposure entrance port for the lateral projection, the skin dose was 17 mGy. The lower lateral projection skin dose was due to the introduction of copper filtration, which is automatically controlled by the angiography system. Note that the peak skin dose for all 3D RA acquisition modes was significantly lower than the peak skin dose for biplanar DSA. For the standard 3D RA acquisition used at our facility (3D-H 8S), the peak skin dose was approximately 25% of the peak skin dose for biplanar DSA.

Cumulative Incident Dose

The cumulative incident dose for 3D RA acquisition modes and biplanar DSA are also listed in Table 3. As with 3D RA peak skin dose values, the high-dose-mode acquisitions are approximately 2.3 times higher in cumulative incident dose than low-dose modes and the cumulative incident dose increases
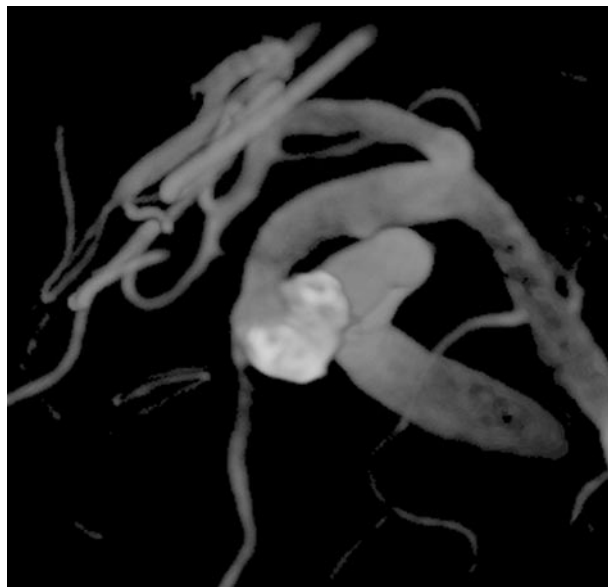

FIG 2. Volume-rendered 3D RA image after coil embolization of a complex left ophthalmic aneurysm. On biplanar angiography, the coil mass overlapped the parent vessel in both views. The lumen was easily viewed on the reconstructed 3D RA image. During embolization, we used serial 3D RA runs to assess whether each additional coil compromised the lumen of the parent artery.

proportionally with rotation arc duration. Note that the 3D RA cumulative incident dose is higher than the peak skin dose by a factor of 2.2–2.5 for all acquisition modes. This is expected, because the cumulative incident dose value includes all the exposed entrance skin surface. For biplanar DSA, the cumulative incident dose is slightly lower than the peak skin dose, even though the cumulative incident dose value combines the frontal and lateral exposure. This relationship is consistent with the fact that the cumulative incident dose value does not include tissue backscatter. For the standard 3D RA acquisition mode, the cumulative incident dose was 36% of the cumulative incident dose for biplanar DSA. Because the 3D RA entrance dose area is spread over a larger region of the head, the reduction in peak skin dose is more significant than the reduction in cumulative incident dose.

Discussion

Contrary to what might be expected from consideration of the total image acquisition count only, the patient radiation dose for a 3D RA acquisition is lower than a biplanar DSA series. This is true for both deterministic radiation effects and, to a lesser degree, stochastic effects. This result has a direct impact on patient care decisions, particularly for complex aneurysms where 3D RA provides improved delineation of aneurysm morphology as compared with biplanar DSA. For example, the aneurysm depicted in Fig 2 curves around the adjacent artery in a C shape, making it difficult to delineate in DSA projection views.

Visualization of this aneurysm during embolization was greatly enhanced by the use of multiple 3D RA acquisitions, which could be incorporated into the procedure without excessive patient radiation dose.

Furthermore, there is a potential for significant patient radiation dose savings when a 3D RA acquisition is used in place of 1 or more biplanar DSA series in a interventional neuroradiology procedure. Abe et al (2) reported that the use of 3D RA resulted in a reduction in the number of DSA series required for cerebral aneurysm treatment procedures. On average, the addition of 2 3D RA acquisitions eliminated 6 full DSA series—used to define the working projection—and 4 control DSA series—used to assess progress of treatment during embolization. On the assumption that a control DSA series results in half the dose of a full DSA series, this substitution would represent a peak skin dose reduction of 405 mGy and a cumulative incident dose reduction of 330 mGy for the 3D-H 8S acquisition mode. On the basis of a recently published patient dose survey (9), the median peak skin dose for cerebral aneurysm embolization procedures was found to be 2800 mGy. (Note that the typical threshold skin dose for deterministic effects is 2000 mGy [14]). In light of the reduction in DSA series specified above, the use of 3D RA reduced the peak skin dose by approximately 15%.

In this study, the 3D RA dose was measured for a subtracted acquisition, which includes both mask and contrast rotational arcs. Unsubtracted 3D RA reconstructions are also possible and reported to provide useful clinical information (19). The advantages of unsubtracted 3D RA include elimination of misregistration artifact from subtraction, reduction of motion artifacts, and visualization of interventional materials and bone along with contrast-filled vessels. Relative to patient radiation dose, unsubtracted 3D RA requiring image acquisition during only 1 rotational arc results in a reduction by half in peak skin dose and cumulative incident dose as compared with subtracted 3D RA.

It is important to note that peak skin dose for biplanar DSA can reach higher levels if frontal and lateral entrance exposure regions overlap. For the typical geometric configuration used in this study, the frontal and lateral exposure fields were found to be distinct but quite close. It is reasonable to expect that slight changes in II FOV, collimation, angulation, and patient size could result in exposure field overlap with significantly higher peak skin doses. In addition, other modifications in DSA acquisition technique also affect patient dose, including the air gap between the patient and the image intensifier, the dose mode selection and variations in copper filtration thickness (20). Variations in these parameters, plus variations in 3D RA acquisition methods used by different angiography system manufacturers, require that specific measurements be made to determine accurate DSA and 3D RA dose values for each unique configuration.

Conclusions

Although 3D RA requires the acquisition of many more images than a typical biplanar DSA run, the patient radiation dose for 3D RA is considerably lower: nearly a factor of 4 lower in peak skin dose and 40% lower in cumulative incident dose. There is a potential for significant patient radiation dose savings if 3D RA acquisitions are substituted for 1 or more biplanar DSA runs during interventional neuroradiology procedures.

References

1. Klucznik RP. **Current technology and clinical applications of three-dimensional angiography.** *Radiol Clin North Am* 2002;40:711–728
2. Abe T, Hirohata M, Tanaka N, et al. **Clinical benefits of rotational 3D angiography in endovascular treatment of ruptured cerebral aneurysms.** *AJNR Am J Neuroradiol* 2002;23:686–688
3. Albuquerque FC, Spetzler RF, Zabramski JM, et al. **Effects of three-dimensional angiography on the coiling of cerebral aneurysms.** *Neurosurgery* 2002;51:597–605
4. Anxionnat R, Bracard S, Ducrocq X, et al. **Intracranial aneurysms: clinical value of 3D digital subtraction angiography in the therapeutic decision and endovascular treatment.** *Radiology* 2001;3:799–808
5. Castano-Duque CH, Ruscalleda-Nadal J, De Juan-Delago M, et al. **Early experience studying cerebral aneurysms with rotational and three-dimensional angiography and review of CT and MR angiography literature.** *Interv Neuroradiol* 2002;8:377–391
6. Hochmuth A, Spetzger U, Schumacher M. **Comparison of three-dimensional rotational angiography with digital subtraction angiography in the assessment of ruptured cerebral aneurysms.** *AJNR Am J Neuroradiol* 2002;23:1199–1205
7. Missler U, Hundt C, Wiesmann M. **Three dimensional reconstructed rotational DSA in planning treatment of intracranial aneurysms.** *Eur Radiol* 2000;10:564–568
8. Sugahara T, Korogi Y, Nadashima K, et al. **Comparison of 2D and 3D digital subtraction angiography in evaluation of intracranial aneurysms.** *AJNR Am J Neuroradiol* 2002;23:1545–1552
9. Gkanatsios NA, Huda W, Peters KR. **Adult patient doses in interventional neuroradiology.** *Med Phys* 2002;29:717–723
10. Kemerik GJ, Frantzen MJ, Oei K, et al. **Patient and occupational dose in neurointerventional procedures.** *Neuroradiology* 2002;44:522–528
11. O'Dea TJ, Geise RA, Ritenour ER. **The potential for radiation induced skin damage in interventional neuroradiological procedures: a review of 522 cases using automated dosimetry.** *Med Phys* 1999;26:2027–2033
12. Miller DL, Balter S, Cole PE, et al. **Radiation doses in interventional radiology procedures: the RAD-IR study. Part I. Overall measures of dose.** *J Vasc Interv Radiol* 2003;14:711–727
13. Miller DL, Balter S, Cole PE, et al. **Radiation doses in interventional radiology procedures: the RAD-IR study. Part II. Skin dose.** *J Vasc Interv Radiol* 2003;14:977–990
14. US Food and Drug Administration. **FDA advisory: avoidance of serious X-ray skin injuries during fluoroscopically-guided procedures, Center for Devices and Radiological Health, U.S. Food and Drug Administration.** September 30, 1994
15. International Commission on Radiological Protection. **Avoidance of radiation injuries from medical interventional procedures. ICRP publication 85.** *Ann ICRP* 2000;30:7–67
16. De Sousa MC, Aubert B, Ricard M. **Evaluation of physical performance of a scintillation dosemeter for patient dosimetry in diagnostic radiology.** *Br J Radiol* 2000;73:1297–1305
17. Wagner LK, Pollock JJ. **Real-time portal monitoring to estimate dose to skin of patients from high dose fluoroscopy.** *Br J Radiol* 1999;72:846–855
18. International Electrotechnical Commission. *Medical electrical equipment. Part 2–43. Particular requirements for the safety of x-ray equipment for interventional procedures.* IEC 60601–2-43. Geneva, Switzerland: International Electrotechnical Commission, 2000
19. Hirai T, Korogi Y, Suginohara K, et al. **Clinical usefulness of unsubtracted 3D digital angiography compared with rotational digital angiography in the pretreatment evaluation of intracranial aneurysms.** *AJNR Am J Neuroradiol* 2003;24:1067–1074
20. Wagner LK, Archer BR, Cohen AM. **Management of patient skin dose in fluoroscopically guided interventional procedures.** *J Vasc Interv Radiol* 2000;11:25–33